7 CAN FLAX REPLACE E-GLASS IN STRUCTURAL COMPOSITES? A SMALL WIND TURBINE BLADE CASE STUDY*

7.1 Introduction

Plant fibre reinforcements, particularly if used in combination with a degradable polymer matrix, are perceived to serve as inexpensive and highly renewable alternatives to traditional synthetic fibres. As E-glass fibres dominate today's FRP market (Fig. 1.1) [1] and as plant fibres offer several technical advantages over Eglass (Table 1.1), the former have been marketed as potential substitutes to the latter. Indeed, the composites industry has seen a growing usage of plant fibre reinforced composites in recent years; albeit for predominantly non-structural automotive applications [2, 3] and replacing primarily wood fibre reinforced composites [4]. The current applications of plant fibre composites (PFRPs) have been listed in *Chapter 1*. Despite the historic use of PFRPs in structural components, such as the exterior body of automotives [5, 6] and the fuselage of military aircrafts [5, 7], and the promising mechanical properties of cellulose [2], the uptake of PFRPs by industry in structural applications has been limited [5]. This is attributable to the fact that the impressive theoretical properties of plant fibres have been difficult to exploit in practice. The major issues impeding the wide-spread use of PFRPs, in both non-structural and structural application, have been discussed in *Chapter 2*.

Nonetheless, an interest, at least in the scientific community, has lingered on the development and potential use of PFRPs for performance-demanding applications. For the certification of a structural component, both small-scale specimen tests and full-scale tests are acceptable as proof of component structural integrity (Fig. 7.1).

Shah DU, Schubel PJ, Clifford MJ. Can flax replace E-glass in structural composites? A small wind turbine blade case study. *Composites Part B: Engineering*, 2013, 52: p. 172-181.

DU Shah Page | 201

^{*} This chapter is based on the peer-reviewed journal article:

However, the safety factors associated with the former are significantly greater than the later. For instance, small wind turbine (SWT) blades designed only through limit state (ultimate strength) analysis based on small-scale specimen tests require a safety factor of 9.0, while blades designed and subsequently tested in a full-scale (ultimate strength) test require a safety factor of 3.3 [8]. Although there has been serious headway in developing PFRPs for structural applications (*e.g.* [9-11]), investigations are at lab-scale coupon tests. To date, there are only limited, if any, scientific studies that conclusively show the suitability of PFRPs over E-glass reinforced composites (GFRPs) for structural applications at a full-scale level [5]. Using the findings of this thesis thus far, this study aims to demonstrate whether PFRPs are potential structural replacements for GFRPs, through full-scale testing of a composite structure.

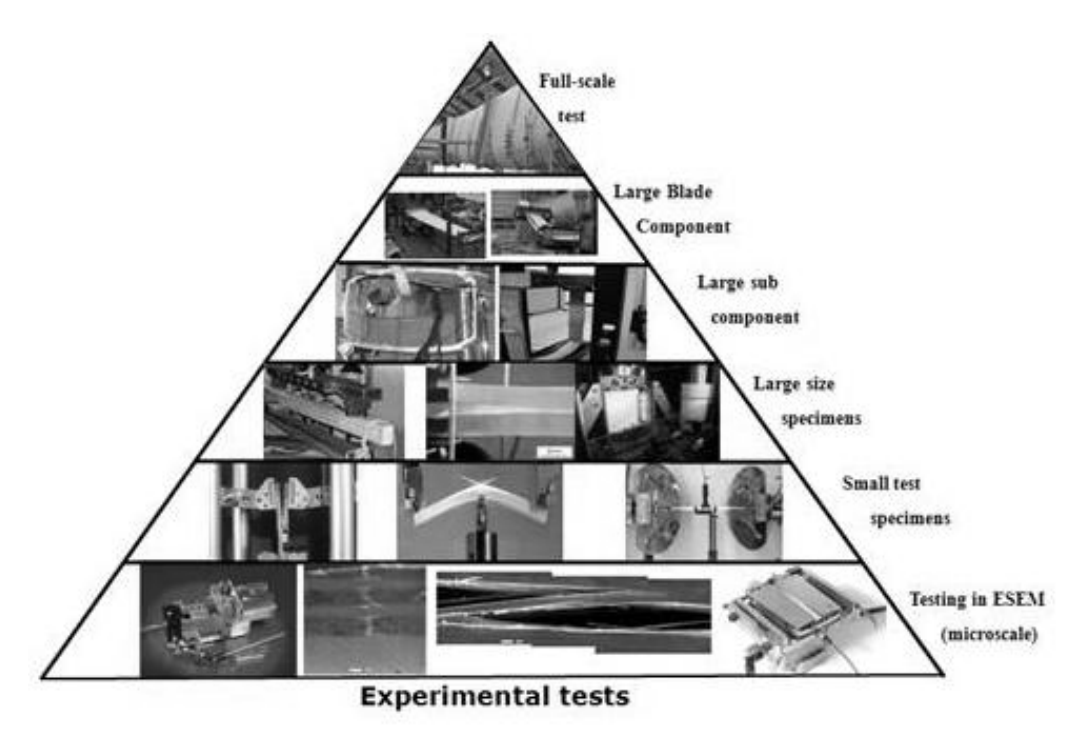


Fig. 7.1. Certifying agencies accept both small-scale tests and full-scale tests as proof of component structural integrity [12].

7.1.1 Reinforcements for rotor blades: plant fibres or E-glass?

GFRPs are by far the most widely used material for rotor blade manufacture. In recent years, carbon fibre has become of increasing interest due to the structural demands of ever-larger blades and the decreasing price of carbon fibres. Nonetheless,

natural or bio-based materials are of potential interest as rotor blade materials, due to their moderate mechanical performance and attractive environmental profile [13]. While wood was one of the first materials for rotor blades, today wood epoxy laminates are a less frequent but not an uncommon material for rotor blades; indeed a large material database exists, accredited by certification standards [8], to support their utilisation. However, the design limitations with using wood, its low stiffness and high variability in quality, alongside the higher performance capacity of GFRPs, give wood-based materials a tough run.

PFRPs may be more suitable to compete against GFRPs. Over the past five years, some researchers have attempted to evaluate the potential of PFRPs specifically for wind turbine blade applications. Brondsted et al. and their group [14, 15] extensively studied the mechanical properties of bamboo/epoxy laminates, aiming to develop bamboo composites for large (>1 MW) turbine blades. They concluded that bamboo composites had higher strength, stiffness, fatigue life and fracture toughness than wood [14]. They also compared the sustainability of a bamboo blade against a GFRP blade through qualitative life cycle analysis and suggested that bamboo composites are a more environmentally-friendly option than GFRPs [15]. However, Brondsted et al. did not manufacture or test a full-scale biocomposite blade. Frohnapfel et al. [16] produced small vertical axis wind turbine blades using woven flax reinforcements. Note that rotor blades for vertical axis turbines observe much lower loads than those faced by rotor blades for horizontal axis turbines. This is because the load-bearing members in vertical axis turbines are the cross-members holding the blade. Nonetheless, Frohnapfel et al. [16] demonstrated that a 1.2 m flax blade, manufactured via press-moulding, successfully met the static test requirement (with a 2.5 times safety factor). However, their attempt at manufacturing a larger 3 m flax blade, via vacuum infusion, was unsuccessful. More recently, aiming to produce a wind turbine car, Mikkelsen et al. [17, 18] investigated the possibility of manufacturing 0.6 m long flax and flax/carbon hybrid blades. Through mechanical tests, they found that although an optimised hybrid blade with a dominating amount of flax fibres performed as well as the pure carbon blade, the pure flax blade performed poorly. The masses of the manufacture carbon, carbon/flax and flax

blades were 0.26 kg, 0.31 kg and 0.56 kg. Mikkelsen *et al.* [17] estimated that the embodied energy of the flax blade was 40% lower than that of the carbon blade.

The Wind Energy Materials Group (within the Polymer Composites Research Group) at The University of Nottingham has been involved with the design and manufacture of wind turbine blades. The Group is currently working on an 11 kW horizontal axis 3-bladed turbine with a rotor diameter of 7 m. In particular, through this NIMRC funded research project, the Group has been investigating the potential of sustainable plant fibre reinforcements as a replacement to conventional E-glass reinforcements in small wind turbine (SWT) blades. A small wind turbine is classified as one with a rotor diameter < 16 m or rated capacity < 100 kW [8]. This investigation has large implications owing to the unprecedented growth of the global SWT industry (Fig. 7.2). It is estimated that by 2020, the total UK small wind capacity will exceed 1300 MW, through the installation of more than ~400,000 SWTs [19]. Assuming these are 3-bladed systems, more than 1 million blades will need to be manufactured [19].

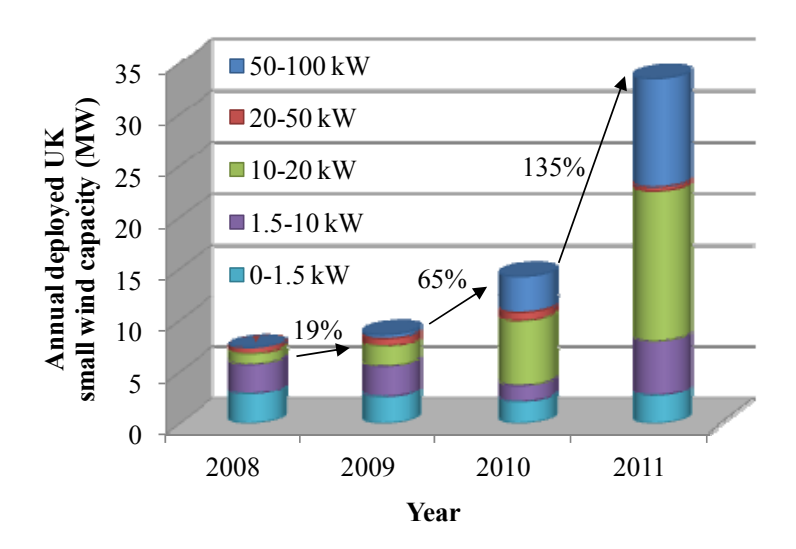


Fig. 7.2. Annual deployed UK small wind system capacity (MW). Data for 2011 is based on manufacturing forecasts. Adapted from [19].

The blades of a wind turbine are a critical and costly component of a wind turbine system. Having a service life of 20–30 years and cycling in excess of 200 rpm, small rotor blades are designed against several major structural conditions including strength, stiffness and tip deflection during operational loading (design wind speeds

of 11.9 ms⁻¹) and severe loading (extreme wind speeds of 59.5 ms⁻¹), as well as very high numbers of fatigue cycles (> 10⁹ cycles) during service.

The loads on a rotor blade can be categorised as aerodynamic loads (such as drag, lift and shear), inertial loads (such as gravitational, gyroscopic, centrifugal) and operational loads (resulting from turbine control such as yawing, pitching). These are depicted in Fig. 7.3. Typically, gravitational loads are insignificant for small blades. As shown in Fig. 7.3, the loads can be divided into three directions: flap-wise (bending the blade downwind), edge-wise (bending the blade in the rotational direction) and axial (along the blade length) directions. For small blade, the flap-wise loads are significantly larger than the axial loads and edge-wise loads.

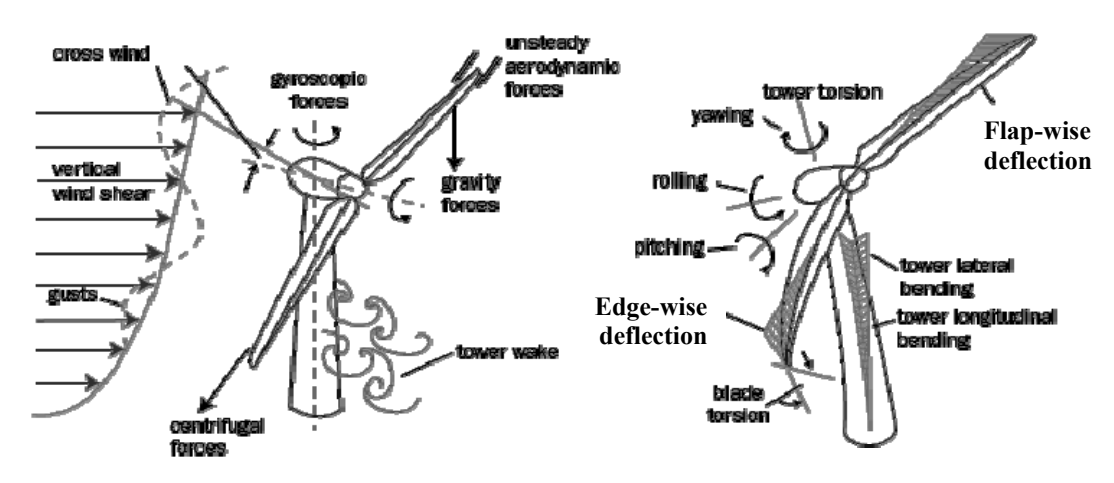


Fig. 7.3. The blades of a wind turbine system experience various loads [20].

Naturally, for certification of the SWT blades, the structural integrity of the blade needs to be demonstrated by analysis and full-scale mechanical tests, as per BS-EN 61400-2:2006 [8] and BS-EN 61400-23:2002 [21]. Recently, the author of this thesis has shown [22, 23], using fatigue data based on lab-scale coupon tests (*Chapter 6*) and combining the flap-wise, edge-wise and axial design blade loads into pure tensile/compressive loads (see Fig. 7.4), that a PFRP (hemp/polyester) SWT blade can survive the design fatigue loads (inclusive of a 1.50 safety factor) for the required 20-year design life.

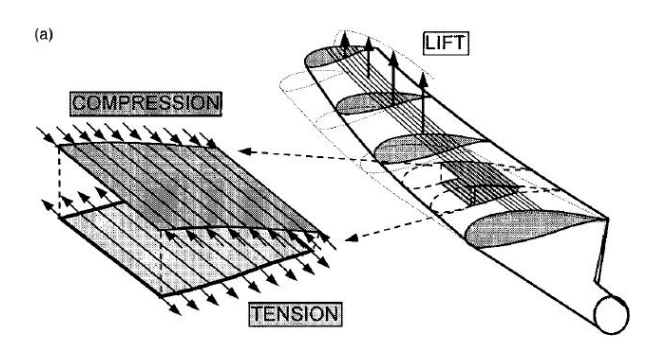


Fig. 7.4. For simplified fatigue analysis, the axial, flap-wise and edge-wise loads can be translated into tension/compression loads along the blade length [24].

This chapter details a comparative case study looking at the manufacture, analysis and mechanical testing of 3.5 m composite rotor blades (suitable for an 11 kW SWT) built from flax/polyester and E-glass/polyester. Firstly, this chapter compares the manufacturing properties, weight, cost, and sustainability of the two blades. Secondly, through static flap-wise testing of the blades (in accordance to certification standards [8, 21]), their mechanical properties are compared. It is eventually confirmed that like the E-glass/polyester blade, the flax/polyester blade satisfies the design and structural integrity requirements for an 11 kW turbine. Hence, flax can potentially replace E-glass in this structural application.

7.2 DESIGN AND MANUFACTURE OF BLADES

7.2.1 Blade design summary

The study blade is 3.50 m in length, with an average chord length of 0.29 m. For improved blade efficiency, an aerodynamically optimised blade shape, generated through an in-house developed design software (*BladeShaper v2.0*) considering *i*) blade element momentum theory including wake rotation, *ii*) turbine performance, and *iii*) part manufacturability, was employed.

To achieve the desired structural performance, based on past experience, a conventional blade construction is used (Fig. 7.5). The blade consists of a CNC machined core and fibre reinforced composite structural blister caps and constant-thickness outer shell. The core provides resistance against buckling, the

unidirectional fibre reinforced blister caps provide maximum axial (tensile) and bending (flexural) stiffness and strength, and the multiaxial fibre reinforced outer skin provides resistance against torsion-related shear loads. The composite material has a nominal fibre volume fraction of 32-38%. The ratio of multiaxial reinforcement (in the shell) to unidirectional reinforcement (in the blister caps) is ~180-250 wt%.

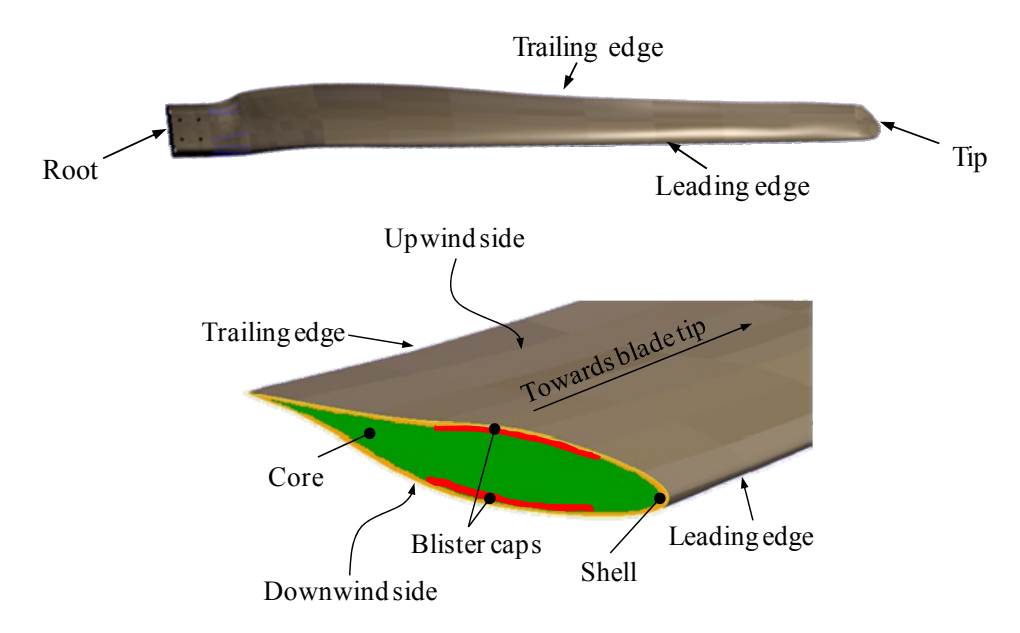


Fig. 7.5. Profile and lay-up of the composite blades.

7.2.2 Blade manufacture

7.2.2.1 Reinforcement materials and their properties

Two identical blades were manufactured using flax and E-glass as reinforcements, employing the same stacking sequence. Low-twist (20 tpm, 400 tex) flax rovings (referred to as F20 in *Chapters 3 and 6*) were sourced from Safilin (France) and produced into aligned (unidirectional (300 gsm) and multi-axial (600-900 gsm)) stitched mats by Formax (UK) Ltd. Aligned E-glass stitched fabrics (300-900 gsm) were also sourced from Formax (UK) Ltd.

The justification behind selecting the plant fibre reinforcement F20 is as follows. In *Chapters 3 and 6*, it was shown that F20 composites exhibit best mechanical properties (static and fatigue) amongst all the PFRPs studied. For the manufacture of

the plant fibre blade and to realise the true structural potential of plant fibres, an optimised reinforcement form (*i.e.* aligned fabrics from F20 low-twist flax rovings) has been selected. Bast fibres in the form of flax are employed, as they are characteristically useful as composite reinforcements. The flax fibres have undergone (field/dew) retting, which is necessary for high fibre quality, and are at least 25 mm in length, ensuring high fibre aspect ratios and length efficiency factors. During roving production, the flax fibres have also undergone caustic soda treatment, implying possibly improved fibre/matrix adhesion and thus load transferring capabilities. Furthermore, low-twist rovings are used so that a continuous reinforcement product could be utilised for preform manufacture, with negligible detrimental effects of yarn twist on composite properties. In addition, the use of aligned fabrics (unidirectional and multi-axial) ensures that the fibre properties are being transferred and utilised where necessary. The nominal fibre volume fractions employed (32-38%) are also much above the estimated critical fibre content (~10%).

To illustrate the difference in mechanical performance of the F20 flax reinforcement and the E-glass reinforcement, Table 7.1 presents the tensile, compressive and fatigue properties of polyester composites made from the unidirectional and biaxial reinforcements (evaluated in *Chapter 3-6*). To assess the comparative performance of the two materials, material performance indices (from *Chapter 2*) are reintroduced here as a form of design criteria. The blade has a sandwich construction (Fig. 7.5) such that it can be assumed that the fibre reinforced plastic material in the shell and blister caps experience pure tension and pure compression (Fig. 7.4). The useful material performance indices are shaded in Table 7.1.

Comparing the tensile properties, it is evident that the relative performance of unidirectional flax composites to unidirectional E-glass composites is similar to the relative performance of biaxial flax composites to biaxial E-glass composites. For instance, the specific tensile stiffness of both unidirectional and biaxial flax composites is ~65% that of unidirectional and biaxial E-glass composites, respectively. The tensile material performance indices for the blade are specific stiffness (E/ρ) and specific strength (σ/ρ) . Notably, F20 composites have a comparable (up to 87%) specific stiffness to GFRP; this is also reflected by the back-

calculated fibre modulus, where flax exhibits a stiffness of 68 MPa. On the other hand, the specific strength of both unidirectional and biaxial flax composites is only ~45% that of unidirectional and biaxial GFRP. Again, the effective fibre strength reinforces this assertion. It is expected, therefore, that for the same mass of material, a flax composite would elongate as much as an E-glass composite, but the flax composite would fail at a significantly lower tensile stress.

From Table 7.1 it is clear that in terms of absolute properties flax composites do not perform as well as they do in tension. E-glass on the other hand, performs only marginally worse in compression; this is one of its well-known advantages [25]. While the compression modulus of unidirectional F20/polyester is 54% that of unidirectional E-glass/polyester, the compression strength of the former is only 32% of the latter. However, the material performance indices reveal a different story. The compressive material performance indices for the blade are specific stiffness ($E^{1/3}/\rho$) and specific strength ($\sigma^{1/2}/\rho$). The specific modulus of F20/polyester is marginally (3%) larger than that of E-glass/polyester, and the specific strength of the former is 70% of the latter. In terms of the material performance indices, flax composites perform better in compression than in tension, and flax composites are more competitive with GFRP in compression. Some researchers [26] have revealed that the compressive properties of elementary flax fibres is approximately 80% of their tensile properties, and this ratio is very high compared to other anisotropic fibres.

Finally, comparing the fatigue performance of unidirectional and biaxial F20 composites with GFRPs (Table 7.1), it is found that the fatigue strength at 10⁶ cycles (the fatigue material performance index for a blade) for flax composites is 40-55% that of GFRP.

The comparison in material properties of the flax and E-glass composites show that GFRPs, on the whole, outperform PFRPs, although the specific stiffness performance of PFRPs may be comparable to GFRPs. In addition, PFRPs compete better with GFRPs in specific compressive properties than in specific tensile properties.

Table 7.1. Tensile, compressive and fatigue properties of unidirectional [0] and biaxial $[\pm 45]$ F20/polyester and E-glass/polyester composites. Material performance indices are shaded.

			Unidirectional			Biaxial		
Property			Flax	E-glass	Flax/E-glass	Flax	E-glass	Flax/E-glass
	Fibre volume fraction	%	30.9	42.8		29.2	28.0	
	Density	gcm ⁻³	1.31	1.79	0.732	1.30	1.61	0.807
	Composite stiffness	GPa	23.4	36.9	0.634	5.70	8.77	0.650
le	Composite specific stiffness	GPa/gcm ⁻³	17.9	20.6	0.869	4.38	5.45	0.804
Tensile	Effective fibre stiffness [†]	GPa	67.6	81.6	0.828	-	-	
T	Composite strength	MPa	277	826	0.335	51.4	139	0.370
	Composite specific strength	MPa/gcm ⁻³	213	461	0.462	39.5	86.3	0.458
	Effective fibre strength [†]	MPa	883	1920	0.460	-	-	
	Composite failure strain	%	1.70	1.90	0.895	3.76	4.12	0.913
	Fibre volume fraction	%	32.5	30.0		N/A [‡]	N/A [‡]	N/A [‡]
Ģ	Density	gcm ⁻³	1.30	1.64	0.793	N/A^{\ddagger}	N/A [‡]	N/A [‡]
SSiv	Composite stiffness	GPa	11.3	21.0	0.538	N/A^{\ddagger}	N/A [‡]	N/A [‡]
Compressive	Composite specific stiffness	GPa ^{1/3} /gcm ⁻³	1.73	1.68	1.03	N/A [‡]	N/A [‡]	N/A [‡]
luc	Composite strength	MPa	101	313	0.323	N/A^{\ddagger}	N/A [‡]	N/A [‡]
Ö	Composite specific strength	MPa ^{1/2} /gcm ⁻³	7.73	10.8	0.717	N/A [‡]	N/A [‡]	N/A [‡]
	Composite failure strain	%	3.44	3.70	0.930	N/A^{\ddagger}	N/A [‡]	N/A [‡]
	Fibre volume fraction	%	26.9	30.0		29.2	28.0	_
igue 0.1)	Density	gcm ⁻³	1.29	1.64	0.787	1.30	1.61	0.807
Fatigue (<i>R</i> =0.1)	Single cycle strength	MPa	236	567	0.416	51.4	139	0.370
	Fatigue strength at 10 ⁶ cycles	MPa	115	204	0.564	22.1	57.3	0.386

[†] The effective fibre properties are 'back-calculated' using the rule of mixtures.

 $^{^{\}ddagger}$ N/A = not measured

7.2.2.2 Fabrication of the blade

The blades were manufactured using an unsaturated polyester resin in a light resin transfer moulding (LRTM) process. Both blades took ~1.5 hrs to infuse showing that using plant fibre reinforcements does not significantly alter infusion times. Post cure was conducted at 40 °C for 2 hr. The manufactured flax/polyester and E-glass/polyester blades are shown in Fig. 7.6. An insightful manufacturing advantage of using flax over E-glass is that the former doesn't cause itching during handling and is non-hazardous if inhaled.



Fig. 7.6. Images of the *a*) flax/polyester and *b*) E-glass/polyester blades.

Note that as the flax reinforcements were in the form of rovings (rather than twisted yarns), they were loose (rather than compact). The bulkiness of the fabric layers implied that closing the tool after placing the fabric was difficult, particularly at the maximum chord length where there is also a large variation in cross-sectional thickness. Nonetheless, as increasing yarn twist has several detrimental effects on PFRP performance (as discussed in *Chapter 5*) including lowered permeability, hindered impregnation, formation of impregnation related voids and significant loss in orientation efficiency; rovings are preferred for PFRP components.

7.2.3 Comparison of mass properties

Fig. 7.7a) shows the difference in mass of the flax and E-glass blades. Weighing at 23.3 ± 0.1 kg, the flax blade is 10% lighter than the E-glass blade (25.8 ± 0.1 kg). Interestingly, the density of the flax reinforcement was measured to be 1.57 gcm⁻³, which is 60% that of E-glass (2.66 gcm⁻³). The reason why the flax blade is only 10%

lighter than the E-glass blade is that the fibre accounts for only 18% and 30% of the flax and E-glass blade masses. Directly comparing the fibre masses allows to appreciate the weight savings that flax provides; while the E-glass blade has 7.7 kg of fibre, the flax blade has only 4.2 kg of fibre. That is, using flax, rather than E-glass, reduces the fibre mass by 45%.

As Fig. 7.7a) illustrates, the mass of the core is identical in both blades and accounts for 32-36% of the blade mass. Interestingly, the resin accounts for 38% of the E-glass blade mass but 46% of the flax blade mass. The intake of 1 kg more resin in the flax blade is possibly due to *i*) the slightly lower volume of fibre (accounting for ~ 0.3 kg of extra resin), and *ii*) a cavity forming over certain regions of the blade (specifically, at the maximum chord length) resulting from the deflection of the mould tool.

Note that the volume of fibre reinforcement used in both blades is similar at 0.0027–0.0029 m³. The fibre volume fraction in the composite part of the blades is calculated to be 23-26% (Table 7.2). The lower fibre weight fraction of the flax composite, compared to the E-glass composite (Table 7.2), is solely due to the difference in densities of the flax and E-glass fibres. Therefore, the difference in fibre weight fraction cannot be avoided (if the composites have the same fibre volume fraction).

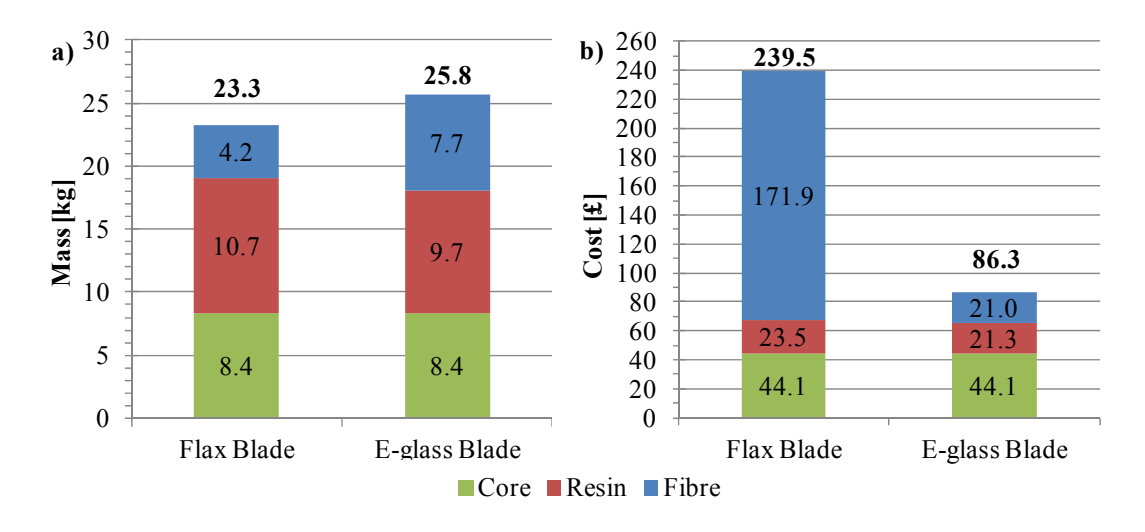


Fig. 7.7. Comparison of the *a*) mass and *b*) materials cost of the flax and E-glass blades.

The centre of gravity C_g from the blade root is 1.26 ± 0.01 m for the flax blade and 1.29 ± 0.01 m for the E-glass blade. The C_g is fairly similar for both blades, as the blade construction and fabric stacking sequence is identical.

Table 7.2. Calculated overall fibre weight and volume fractions in the composite part of the blades (excluding the core).

	Flax blade	E-glass blade
Density [gcm ⁻³]	1.28	1.59
Fibre weight fraction [%]	28.2	44.3
Fibre volume fraction [%]	22.9	26.4

7.2.4 Comparison of materials cost

Fig. 7.7b) presents the difference in materials cost of making the flax and E-glass blades. The materials cost for the flax blade amounts to £239.48, making it approximately 3 times more expensive than the E-glass blade (£86.34). The material cost of the foam core (5.28 £/kg) and the polyester resin (2.20 £/kg) are almost identical for the two blades, amounting to ~£65. Fig. 7.7 shows that despite requiring less fibre in a flax blade, the fibre cost of the flax blade is 8 times that of the E-glass blade. Hence, it is the cost of the fibre reinforcement which is causing the cost disparity between the flax and E-glass blades.

Unlike E-glass, costs of flax reinforcements increase tremendously with processing steps. This is because *i*) E-glass reinforcements are an established mature market, and *ii*) the processing (and incurred costs) of flax and E-glass reinforcements is different. As Table 7.3 highlights, under current market conditions, aligned flax reinforcements are more expensive than aligned E-glass reinforcements at every stage: raw fibre, yarn/roving and aligned fabric. Raw flax itself is barely cost-competitive against raw E-glass [27, 28]. Interestingly, the cost of non-woven mats of flax fibres is comparable to (or even lower than) that of E-glass (Table 7.3). This is possibly a result of the fact that naturally discontinuous plant fibres are readily (without much processing) useable in the production of non-wovens. It is thus not surprising that current industrial applications of PFRPs are principally based on non-woven precursors [3]. However, to make aligned fabric reinforcements, staple plant fibres like flax need to be first processed into yarns/rovings, unlike E-glass which is a

synthetic filament. Flax rovings/yarns are up to 10 times more expensive than E-glass. Madsen *et al.* [29] have also commented on the high market price of such plant fibre yarns. In addition, the actual cost associated with aligned fabric manufacture needs to be accounted. The flax reinforcements were specially produced for this study; the costs for the multi-axial fabrics (300–600 gsm) ranged from 13.8 £/m² to 22.0 £/m². E-glass fabrics (300–600 gsm) were off-the-shelf items, which typically cost 1.80 £/m². By weight, the cost of aligned flax fabric is 6–15 times greater than that of aligned E-glass fabric. In essence, the development of low-cost aligned plant fibre semi-products is a critical and potentially limiting factor in encouraging the future industrial use of PFRPs, as an alternative to GFRPs.

Table 7.3. Flax is costlier than E-glass at every stage. Costs for raw fibre, yarn/roving and aligned fabrics are obtained from materials suppliers (and assumed indicative of the market prices) as of Dec 2012. Costs for non-woven mats are from [29].

Cost of reinforcement	Flax [‡]	E-glass	Flax/E-glass	
Raw fibre [£/kg]	1.5	1.3	1.2	
Yarn/roving [£/kg]	10.0-13.0	1.3	7.7-10.0	
Aligned fabric [£/kg]	36.7–45.9	3.0-6.0	6.1-15.3	
Non-woven mat [£/kg]	1.5	2.2	0.7	

[‡] Note that the prices of the flax reinforcements quoted here are based on small quantities and should only be used as guidelines. Prices reduce significantly with higher quantities (> 5 tonnes), but also depend on other factors such as market conditions and fibre quality.

7.2.5 Comparison of eco-impact

In composites manufacture, the embodied energies of the various materials (fibre reinforcement, matrix and core) typically account for over 80% of the total environmental impact of the composite component [30]. The manufacturing process and operations, on the other hand, typically account for less than 15% of the total eco-impact [30]. As the flax and E-glass blade have been manufactured in an identical manner, the eco-impact of replacing E-glass with flax can be gauged by estimating the cumulative embodied energies of the materials in the two blades.

As discussed in *Chapter 2*, based on life cycle assessment studies on plant fibre reinforcements, while the energy required in the cultivation of plant fibres is low (4-

15 MJ/kg [31-35]), further processing steps (*e.g.* retting and spinning) can significantly increase the cumulative energy demand to 54-118 MJ/kg for flax sliver and 81-146 MJ/kg for flax yarn [32-34, 36]. Conversion from slivers/yarns to fabrics would require further energy inputs. The aligned flax fibre fabrics used in this study employ flax rovings; here, it is assumed that the embodied energy of the flax fabrics will be in the range of 54-118 MJ/kg (similar to the flax sliver). On the other hand, the embodied energy of E-glass yarns and fabrics is in the range of 30-55 MJ/kg [34, 35]. Pre-empting the conclusions, it is clear that aligned plant fibre preforms have a larger eco-impact than E-glass preforms. Note however that the eco-impact of component end-of-life disposal is not considered here; while GFRPs are generally landfilled or incinerated (for energy recovery from the resin alone), PFRPs would be incinerated (for energy recovery from both the plant fibres and the resin). Unsaturated polyester resin and foam core have embodied energies of approximately 63-78 MJ/kg [37] and 80-120 MJ/kg [30], respectively.

Using these estimates of embodied energies of the various constituent materials and the quantity of material used in each blade (Fig. 7.7), the cumulative materials embodied energy of the flax and E-glass blade is estimated to be in the ranges of 1573-2338 MJ (or 68-100 MJ/kg) and 1514-2188 MJ (or 59-85 MJ/kg), respectively. In essence, despite requiring 45% less fibre mass, the flax blade has an up to 15% larger eco-impact than the E-glass blade. Certainly, increasing the fibre content in the flax blade (to enhance structural integrity) would result in a much larger eco-impact.

It can also be commented here that perhaps the cost of a product may be a useful indicator of the embodied energy of a product; while raw flax fibres and non-woven mats are low-cost and require low energy for production, aligned plant fibre semi-products are high-cost and require high energy inputs for production. These findings highlight that for structural PFRPs to be projected as environmentally benign alternatives to GFRPs, the development of sustainable processes for the manufacture of aligned plant fibre semi-products is a critical step ahead. Furthermore, it is suggested that as the matrix and core are the other constituents of the blade, which notably make up a larger weight fraction of the blade than the fibre constituent, to truly reduce the eco-impact of the final product, it is essential that not only the fibre

reinforcement but also the matrix and core are bio-based or at least bio-sourced. Indeed, the development of high-performance bio-resins and bio-cores is another critical factor in the wide acceptance of PFRPs as sustainable materials.

7.3 MECHANICAL TESTING OF BLADES

Upon the design and manufacture of the two blades, their structural integrity was assessed through design load analysis and full-scale mechanical tests, as per BS-EN 61400-2:2006 [8] and BS-EN 61400-23:2002 [21]. This section details the flap-wise static testing of the two blades.

7.3.1 Description and derivation of test loads

7.3.1.1 Design loads

The SWT, for which the blades are to be used, is an 11 kW Class-II horizontal axis 3-bladed upwind stall regulated turbine, with a rigid hub, cantilever blades, active yaw mechanism and fixed pitch. Hence, design loads for the blades can be determined using simplified conservative load equations in [8]. For the flap-wise static testing of the blade, as per [21] it is the blade root bending moment M_{yB} (acting to bend the blade tip downwind) that is of interest. [21] acknowledges that stresses caused by radial loads (F_{zB}) are relatively low. This is confirmed through a simple stress analysis at the blade root. At the design wind speed (11.9 ms⁻¹) and design rotor speed (170 rpm) under normal operating conditions (*Load Case A* in [8]), the flax and E-glass blade experience a radial load of 23.6 kN and 26.2 kN, respectively (due to difference in masses). The resultant mean stress at the blade root is only 1.22–1.35 MPa.

Typically, the blade is tested against the calculated blade root bending moment M_{yB} under normal operating conditions (*Load Case A* in [8]) and worst case loading. Note that this turbine has an active yaw mechanism which ensures that when subjected to extreme gusts (*Load Case H* in [8] at extreme wind speed of 59.5 ms⁻¹), the turbine is parked at 90° yaw angle, leading to minimal exposure. Using known values for constants, blade/turbine parameters and wind condition parameters, the design loads on the blade have been determined for the several load cases [38]. For this particular

turbine setup, the worst case loading was found to occur when there is a yaw error of 30° (*Load Case C* in [8] at design wind speed of 11.9 ms^{-1}). Conveniently, blade root bending moment M_{yB} at *Load Case A* and *Load Case C* are not a function of blade mass, and hence are the same for both the blades.

7.3.1.2 Target test loads

To determine the target test loads, partial safety factors have to be incorporated with the design loads. In particular, BS-EN 61400-2:2006 [8] and BS-EN 61400-23:2002 [21] require the inclusion of the product of the following partial safety factors: load γ_f , consequence of failure γ_n and blade to blade manufacturing variations γ_s . It appears that the recommended combined safety factor is similar in various certification standards [39].

As is later revealed, a single-point test method is employed, where a single concentrated point load is applied at l m from the blade root. The target point load F $(F = M_{yB}/l)$, associated with the target blade root bending moment M_{yB} , at the normal operation and worst case loads is 1.48 kN and 3.99 kN, respectively.

7.3.2 Experimental set-up

7.3.2.1 Test equipment

For the static flap-bending test, a single point test method was employed. The blade root was fixed to a specially designed rigid steel test rig (Fig. 7.8a)) via a simple bolted connection. No inserts or studs are used; rather, the bolts go through holes in the composite sandwich (skin/cap/core/cap/skin). The test rig mimics the real blade root to hub connection, with the same bolt pattern, plate thickness and plate local geometry. The test rig was attached to two structural poles. The blade was fixed horizontal (flap-wise up) and was loaded by an overhead crane. A composite saddle was specially built to enclose the blade's cross-section at the desired load point (*l* m from the blade root). This is presented in Fig. 7.8b). A rubber lining was placed between the saddle and the blade, to provide grip and to protect the blade from local damage due to a concentrated pressure at the load application point.





Fig. 7.8. Image showing the a) test rig and b) composite saddle.

The overall loading arrangement is presented in Fig. 7.9. The external sleeves of the saddle have eyebolts which are used to connect to a 12 kN calibrated load cell. The load cell rests on a spreader beam and is attached to a 5 tonne overhead crane. As the blade deflects, the load direction relative to the blade orientation can change. To ensure that the load is perpendicular to the load application point on the blade, the overhead crane is periodically moved towards the blade root after releasing some load. A spring-loaded marker, attached at the blade tip, provides in-situ tip displacement monitoring.



Fig. 7.9. Blade flap-wise test loading arrangement.

7.3.2.2 Test regime

To systematically achieve the target point test loads F, a loading sequence was developed (Fig. 7.10). The test has three stages: i) loading up to the 100% normal operation load (F = 1.48 kN), ii) loading up to the worst case load (F = 3.99 kN, i.e. 270% (= 3.99/1.48) of normal operation load), and iii) loading to failure. To ensure steady loading, small steps of 0.01–0.03 kN are used. Regular load dwells are incorporated to allow the blade to settle.

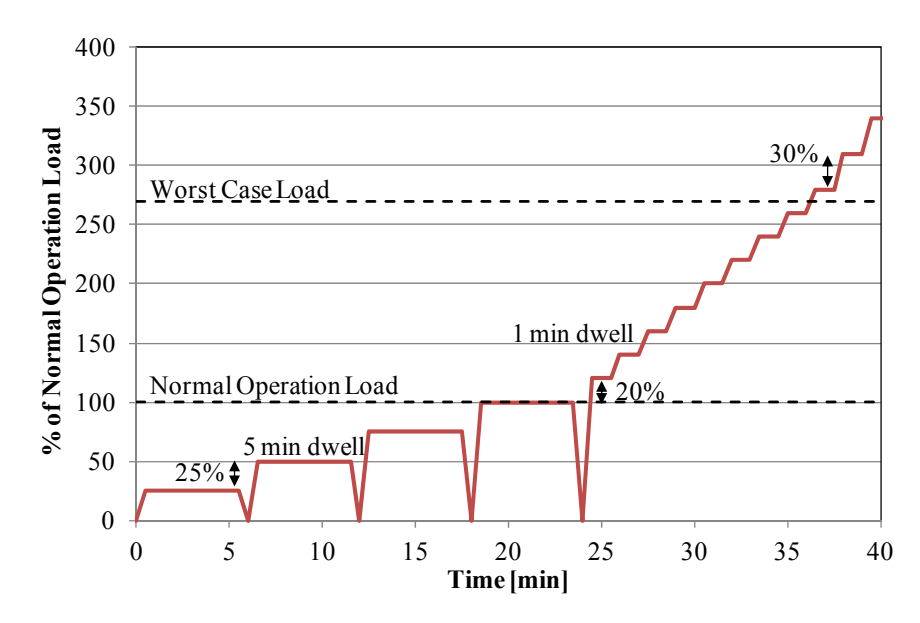


Fig. 7.10. Blade flap-wise test loading regime. Load values (y-axis) are normalised by the normal operation load (of 1.48 kN).

7.3.2.3 Description of failure criteria

To satisfy BS-EN 61400-23:2002 [21], no superficial failure (small cracks, buckling or delamination) should occur below the normal operation load. In addition, no functional failure (substantial loss in functionality through permanent deformation) or catastrophic failure (complete disintegration or collapse) should occur below the worst case load.

7.3.3 Results and discussion

The flax and E-glass blades were subjected to flap-bending tests according to the experimental set-up and loading regime described in Section 7.3.2. Fig. 7.11 presents

graphs of test load and tip displacement as a function of test duration, for both the blades. It is observed that both the blades survive the normal operation load without any superficial failure and survive the worst case load without any functional/catastrophic failure. As both the blades satisfy the ultimate strength requirements of BS-EN 61400-23:2002 [21], the flax blade can be viewed as a potential replacement to the E-glass blade. The failure load and corresponding tip displacement of the flax blade is 4.14 kN and 2300 mm, respectively. The failure data of the E-glass blade is not disclosed. BS-EN 61400-23:2002 [21] does not formally require measuring the failure load and tip deflection.

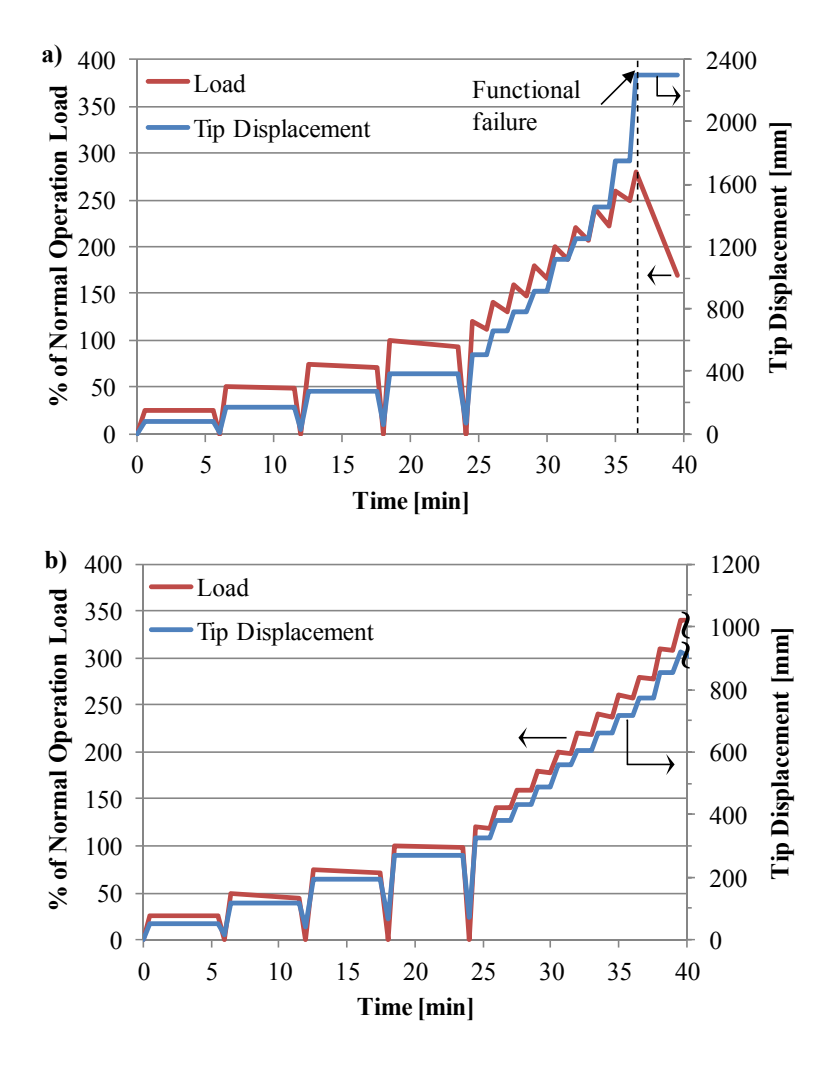


Fig. 7.11. Test load and tip displacement as a function of time, for the *a*) flax and *b*) E-glass blades. The point of functional failure has been indicated. Load values (y-axis) are normalised by the normal operation load (of 1.48 kN).

Table 7.4 presents useful information from the graphs in Fig. 7.11, enabling direct comparison of the performance of the E-glass and flax blades. At normal operation loads, the E-glass blade has a tip deflection of 270 mm while the flax blade has a 40% higher tip deflection of 388 mm. The tip deflections are 8–11% of the blade length. While the flax blade survives the worst case loading like the E-glass blade, the flax blade is significantly more flexible than the E-glass blade. The E-glass and flax blades have a tip displacement of 743 mm and 2025 mm under worst case loading, which is 22% and 60% of the blade length, respectively. To avoid tower strike, BS-EN 61400-23:2002 [21] requires that the tip displacement should be less than the clearance provided between the blade tip and the tower, even at worst case loading. As the traditional practise in designing a turbine is to accommodate the requirements of the blade (i.e. blade-centered design), a turbine can be designed so that a generous clearance is available to accommodate the large tip deflection of the flax blade. A possible design solution is to increase the distance between the rotor centre and tower axis, and use a yaw drive mechanism (or thicker flanges) to balance the increased overturning moment of the rotor. In addition, a modified flax blade design incorporating a spar (with shear webs/caps) will enable major reductions in tip deflection by increasing the flexural rigidity of the blade.

Table 7.4. Loads and corresponding tip displacements of the flax and E-glass blades, at the end of test stages 1, 2 and 3.

	Flax blade				E-glass blade			
	Load		Tip displacement		Load		Tip displacement	
Stage of test loading	kN	% of NO [†] load	mm	% of blade length	kN	% of NO [†] load	mm	% of blade length
Normal operation	1.48	100	388	11	1.48	100	270	8
Worst case	3.99	270	2025	60	3.99	270	743	22
Failure	4.14	280	2300	68	N/A [‡]	N/A^{\ddagger}	N/A [‡]	N/A [‡]

[†] NO load is 'normal operation' load.

The load curves in Fig. 7.11 show relaxation in loads during dwells. It is observed that load relaxation is much higher in the flax blade than the E-glass blade. In fact, in

[‡] Non-disclosable data.

stage 2, the magnitude of load relaxation averages 0.03 kN for the E-glass blade but 0.18 kN for the flax blade. Interestingly, during periods of load relaxation, the blade tip displacement remains fairly constant. The greater load relaxation in the flax blade implies reducing blade stiffness. This could possibly be due to a poorer fibre/matrix interface resulting in gradual plastic deformation through progressive micromechanical damage mechanisms such as fibre/matrix debonding and pull-out. This is common in PFRPs [40, 41] (shown in *Chapters 3 and 4*). In addition, it has been shown in *Chapter 5* that plant fibre composites have a non-linear stress-strain curve, resulting from a very small elastic strain limit of ~0.15%, implying that plastic deformation from micro-damage occurs very early in the load curve [42].

7.3.3.1 Displacement- load curves

Fig. 7.12 presents tip displacement versus load curves for the flax and E-glass blades. Interestingly, while the tip displacement increases at a constant rate with load (linear growth, $R^2 = 0.996$) for the E-glass blade, the tip displacement increases at an increasing rate with load (quadratic growth, $R^2 = 0.989$) for the flax blade. This is in agreement with the load-displacement curve of the different materials. E-glass composites have a linear load-displacement curve, while plant fibre composites have a non-linear load-displacement curve [10, 42, 43] (Chapter 5). In particular, plant fibre composites exhibit softening (i.e. decreasing stiffness with increasing strain/load) [10]. As demonstrated in Chapter 5, the stiffness of flax/polyester composites reduces by up to 30% in the 0-0.25% strain range, while the stiffness of E-glass composites is fairly constant. These observations highlight the differing stress-strain accumulation and damage-growth mechanisms in E-glass reinforced composites and plant fibre reinforced composites, particularly due to the differing fibre structure and morphology and fibre/matrix interactions. It is thought that the non-linear stress-strain curve of the plant fibres, resulting from progressive reorientation of cellulose microfibrils and visco-elasto-plastic deformation of the hierarchal cell wall structure, is translated into the PFRP component [10, 42, 43] (as discussed in Chapter 5).

Fig. 7.12 clearly demonstrates the significantly higher deflection of the flax blade in comparison to the E-glass blade. Fig. 7.12 also presents images of the flax blade under *i*) no load, *ii*) normal operation load, *iii*) worst case load, and *iv*) failure load.

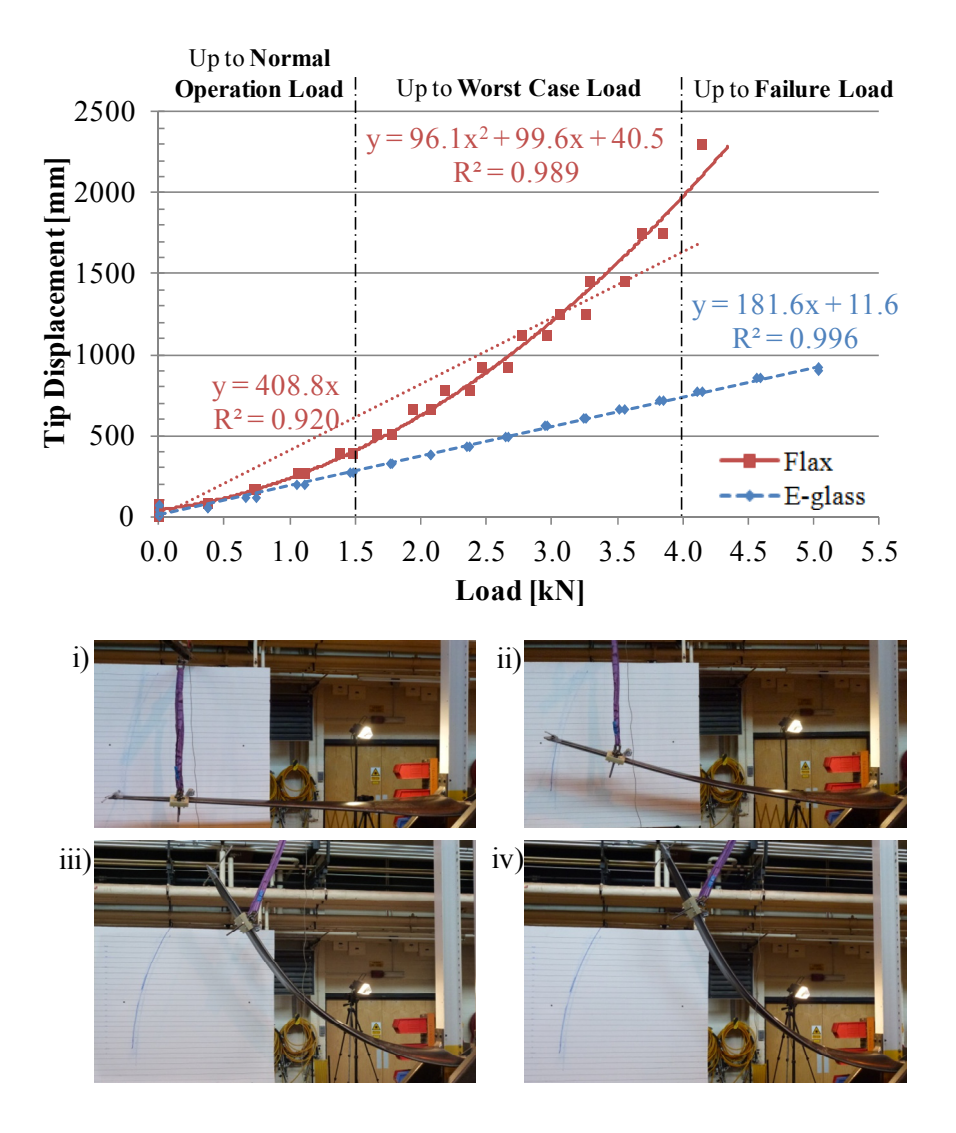


Fig. 7.12. Tip displacement versus load curves for the flax and E-glass blades. Images of the flax blade under *i*) no load, *ii*) normal operation load, *iii*) worst case load, and *iv*) failure load, are also presented.

7.3.3.2 Flexural rigidity of blades in the flap-wise direction

Two strategies are available to estimate the flexural rigidity (EI) of a blade. The first technique involves assuming that the blade can be considered as a uniform cross-section cantilever beam subjected to a single concentrated load at I m from the blade

root. Assuming small deflections and applying appropriate boundary conditions at the ends of the cantilever beam, a simple static analysis using Macaulay's method (Eq. 7.1) can be conducted to estimate the mean flexural stiffness EI_{mean} of the blade (In Eq. 7.2). In Eq. 7.2, y_{tip}/F is the slope of the tip displacement–load curve, z_{tip} (= 3.395 m) is the length of the blade and l is the distance between the point of load application along the blade from the blade root. This simple analysis conveniently shows that the blade flexural stiffness is inversely proportional to the slope of the tip displacement to load curve.

$$EI_{mean} \frac{d^2 y}{dz^2} = M; M = F([z-l]-[z]+l)$$
 Eq. 7.1

$$EI_{mean} = \frac{K}{y_{tip}/F}, \quad K = \frac{[z_{tip} - l]^3}{6} - \frac{z_{tip}^3}{6} + \frac{lz_{tip}^2}{2}$$
 Eq. 7.2

Using the slope (y_{tip}/F) of the linear tip displacement–load curve for the E-glass blade (181.6 mm/kN) and the flax blade (408.8 mm/kN) from Fig. 7.12, and substituting the relevant constants in Eq. 7.2, the mean flexural stiffness EI_{mean} of the E-glass and flax blades is found to be 53.1 kNm² and 23.6 kNm², respectively. That is, the flax blade is 2.25 times more flexible than the E-glass blade. As the displacement-load curve for flax is non-linear and follows a quadratic equation better, a better approximation of EI_{mean} can be obtained if the differential of the quadratic best-fit equation (in Fig. 7.12) is taken as y_{tip}/F . The mean flexural stiffness EI_{mean} of the flax blade is then a function of load, and is found to reduce with increasing load. For instance, EI_{mean} at loads of 0 kN, 1.48 kN (normal operation load) and 3.99 kN (worst case load) is 96.9 kNm², 25.1 kNm² and 11.1 kNm², respectively.

An alternate, and more rigorous, method to estimate the flexural rigidity of the blade involves measuring the vertical deflection (using the video footage) of a blade y_i , subjected to say normal operation loads (F = 1.48 kN, M = 4.15 kNm), at various points along the blade length z_i . 18 points along the leading and trailing edges are used for deflection measurement. From the vertical deflections, the bending angle θ

= $\tan^{-1}(dy/dz)$, and bending rate per unit length $d\theta/dz$ can be calculated using finite difference methods. Eq. 7.3 and Eq. 7.4 present the central difference for θ and $d\theta/dz$, respectively. The flexural rigidity at different points along the blade can then be determined by using Eq. 7.5 [44]. The results for the E-glass and flax blades are presented in Fig. 7.13. The curves observed for the 3.5 m flax and E-glass blades of this study, have a similar profile to those found in literature for a larger 7.5 m GFRP wind turbine blade [44].

$$\theta_i = \tan^{-1} \left(\left(\frac{dy}{dz} \right)_i \right) = \tan^{-1} \left(\frac{y_{i+1} - y_{i-1}}{z_{i+1} - z_{i-1}} \right)$$
 Eq. 7.3

$$\left(\frac{d\theta}{dz}\right)_{i} = \frac{\theta_{i+1} - \theta_{i-1}}{z_{i+1} - z_{i-1}}$$
 Eq. 7.4

$$EI = \frac{M}{d\theta/dz}$$
 Eq. 7.5

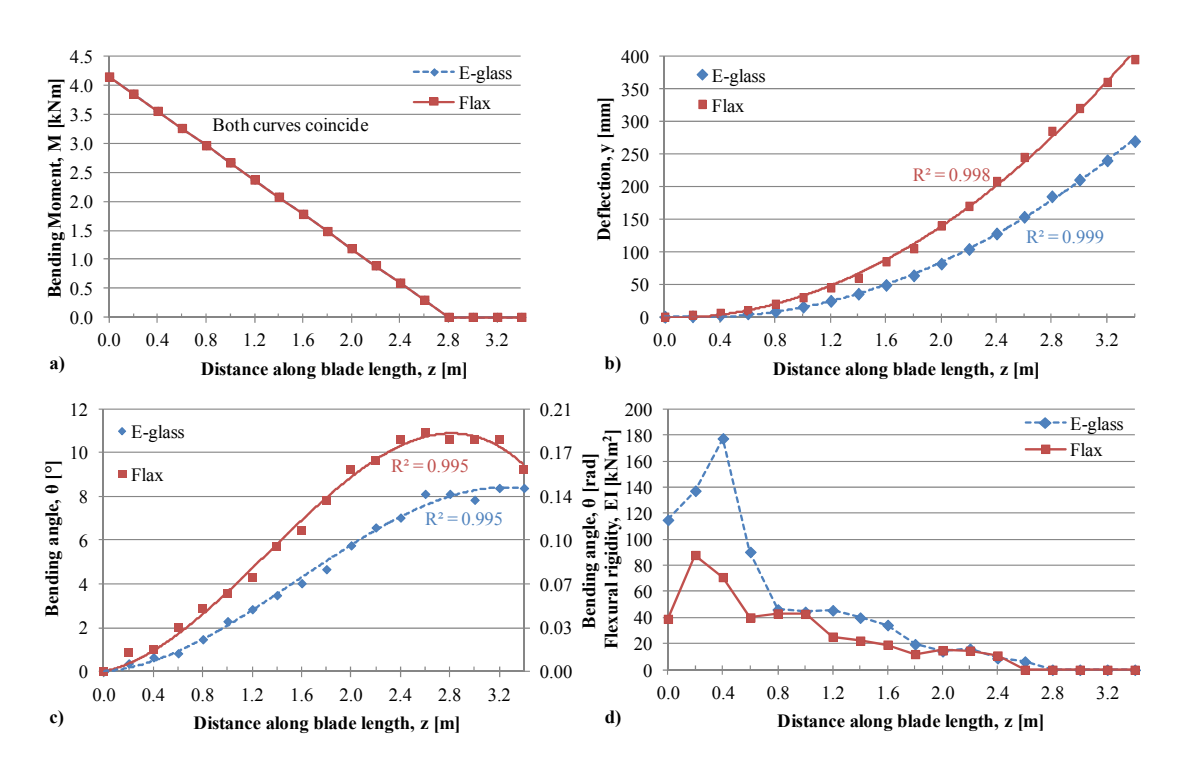


Fig. 7.13. Graphs showing the variation in a) applied moment, b) vertical deflection, c) bending angle and d) flexural rigidity, along the blade length, for the E-glass and flax blades, when subjected to normal operating test loads (F = 1.48 kN).

Fig. 7.13a) shows the applied bending moment M along the blade length z, due to the point load at l m from the blade root. Note that the applied bending moment M is null beyond the load application point. In addition, the bending moment M at the blade root is the required M_{yB} of 4.15 kNm. The resulting vertical deflection along the blade length of the E-glass and flax blades can be observed in Fig. 7.13b). The deflection profile for both blades is observed to follow a quadratic equation ($R^2 > 0.99$). It is clearly observed that the flax blade deflects more than the E-glass blade. The calculated bending angle along the blade lengths for the two blades is presented in Fig. 7.13c). The bending angle is observed to increase fairly linearly up to z = 2.6 m, after which it becomes constant. This is because the load is being applied at l = 2.80 m from the blade root, and beyond this point there is no bending moment (Fig. 7.13a)).

Fig. 7.13d) illustrates the variation in estimated flexural rigidity *EI* along the blade length for both the blades. The higher flexural rigidity at close to the blade root is due to the higher bending moment of area and presence of more layers of unidirectional reinforcement. Sudden dips in the flexural rigidity along the blade length are possibly due to step-changes in the stacking sequence of the blade.

It is observed that the E-glass blade exhibits a higher flexural rigidity at almost all points along the blade length. In particular, the flexural rigidity of the E-glass blade is 2-3 times more than the flax blade, along the first meter of the blade. Using the trapezium rule, an indicative value of the mean flexural stiffness for the blades can be determined. EI_{mean} is found to be 43.4 kNm² for the E-glass blade and 24.6 kNm² for the flax blade. These values are fairly similar to those calculated previously through the simple static analysis method.

7.3.3.3 Comparison of mechanical properties obtained via testing of laminates and full-scale components

Firstly, in comparing the mechanical properties of flax and E-glass composites in Table 7.1, it was found that the tensile and compressive stiffness' of flax composites are between 54-65% that of E-glass composites. The mean flexural rigidity of the flax blade is 57% that of an identical construction E-glass blade. As the flax blade

failed via compressive buckling, perhaps the low absolute compressive stiffness of flax composites in comparison to E-glass composites (also reported in [45]) limits the flexural rigidity of the flax blade. Secondly, the specific stiffness (material performance index) of flax composites is between 80-100% that of E-glass composites (Table 7.1). Comparing the specific flexural rigidity of the flax blade with the E-glass blade (using the density of the composite part of the blades from Table 7.2), it is found that the specific flexural rigidity of the flax blade $(24.6^{1/3}/1.28 = 2.27 \text{ (kNm}^2)^{1/3}/\text{gcm}^{-3})$ is ~100% that of the E-glass blade $(43.4^{1/3}/1.59 = 2.21 \text{ (kNm}^2)^{1/3}/\text{gcm}^{-3})$.

These two observations not only show that the absolute and specific properties of the composites (i.e. flat laminate plaque) are transferred to the blade (i.e. component/structure), but also hint at two important implications. Firstly, the flax blade experiences more deflection than the E-glass blade for the same load due to the comparatively lower absolute stiffness of flax composites. Secondly, the former is the case as the flax blade is 10% lighter than the E-glass blade (fibre mass saving of 45%). Indeed, if the blades were of identical mass and thus density (as blade volume is constant), the stiffness of the flax blade would be comparable to that of the E-glass blade. In essence, there is a critical trade-off between component weight savings and component stiffness; for similar stiffness performance of a flax blade to an E-glass blade, weight savings cannot be achieved. In addition, due to the large difference in densities of flax fibre and E-glass fibre, to achieve the same blade mass (and thus blade density), a considerably higher, and possibly unattainable, flax fibre mass (and thus fibre weight content) would need to be used. For instance, the current fibre mass and blade densities of the flax and E-glass blade are tabulated in Table 7.2. The (composite part of the) flax blade will achieve a maximum density of 1.57 gcm⁻³ for 100% fibre weight fraction (i.e. no resin); the current density (of the composite part) of the E-glass blade, with a fibre weight fraction of only 44.3% is already 1.59 gcm⁻³. It is also noteworthy that using a larger quantity of flax reinforcement would not only reduce weight savings, but would also imply a substantially larger economic cost and eco-impact of the flax blade than is currently the case.

Nonetheless and importantly, this case study demonstrates that despite the well-documented poor strength properties of flax composites in comparison to GFRPs (ratio of 32-37%, Table 7.1), the flax blade, like the E-glass blade, is able to withstand the worst case loads. This shows that more studies are required to critically understand the behaviour of PFRPs when employed in specific applications and structures, rather than limiting materials analysis to data extracted from coupon testing. Indeed, certain applications may be suitable for even low-strength (relative to GFRPs) PFRPs.

7.3.3.4 Failure modes of blades

The E-glass and flax blades failed under different modes, as is depicted by Fig. 7.14 and Fig. 7.15. The E-glass blade failed due to crack formation at the root-hub junction. Upon further loading, the crack grew across the blade cross-section causing extensive delamination. Fig. 7.14 shows how the composite laminates have peeled from the core. The crack eventually grows to such an extent that the trailing edge, along the maximum chord length, split open.



Fig. 7.14. The E-glass blade, failing at the blade root, exhibited extensive delamination.

On the other hand, the flax blade failed ~1 m along the blade length from the blade root (Fig. 7.15a)) which corresponds to a step-change in the stacking sequence. This point of step-change is a possible stress-raiser. Hence, as the load exceeded 4 kN and the tip deflection approached 70% of the blade length, the stress concentration increased substantially. Initially, matrix cracking/peeling was observed (Fig. 7.15b)) – a sign of resin richness. Then, the top surface, experiencing compressive loads,

buckled. The wrinkles and delamination resulting from the compressive failure of the composite laminate can be seen in Fig. 7.15b). Further loading led to complete buckling, delamination and eventually collapse of the blade. The low compressive stiffness and strength of flax composites (Table 7.1) makes compressive buckling an understandably likely source of failure for the flax blade.

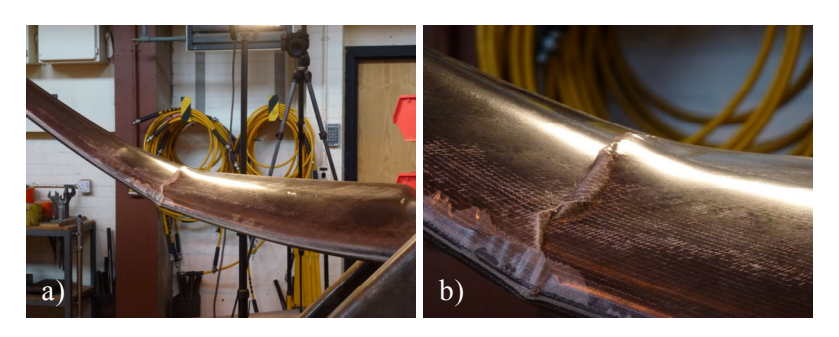


Fig. 7.15. Images of the fractured flax blade during static flap-wise testing showing *a*) the region of failure, and *b*) wrinkle formation due to buckling.

7.4 Conclusions

The objective of this chapter was to demonstrate whether plant fibre composites are potentially structural replacements to E-glass composites. This chapter detailed a novel comparative case study looking at the manufacture and mechanical testing of 3.5 m composite rotor blades (suitable for an 11 kW turbine) built from flax/polyester and E-glass/polyester.

Firstly, this chapter compared the weight, cost, eco-impact and manufacturing properties of the two blades. It is found that although the flax/polyester blade is 10% lighter than the E-glass/polyester blade (fibre mass saving of 45%), the materials cost of the former is almost 3 times that of the latter. Furthermore, comparing the estimated cumulative embodied energy of the flax and E-glass blade, it is found that the flax blade has an up to 15% larger eco-impact than the E-glass blade. Hence, currently, aligned flax reinforcements are a light weight, but not low-cost or sustainable, alternative to conventional aligned E-glass reinforcements.

Secondly, through static testing of the blades (in accordance to certification standards), their mechanical properties were compared. It is confirmed that like the

E-glass/polyester blade, the flax/polyester blade satisfies the design and structural integrity requirements for an 11 kW turbine, under normal operation and worst case loading. Hence, flax is a potential structural replacement to E-glass, particularly for small rotor blade applications.

While the displacement-load curve is linear for the E-glass blade, it is non-linear for the flax blade. This is consistent with the fact that plant fibres and their composites have a non-linear stress-strain curve, while E-glass and its composites have a linear stress-strain curve. This highlights the differing stress-strain accumulation mechanisms in natural materials. The flax and E-glass blades are also found to fail in a different manner. The failure load and corresponding tip displacement of the flax blade is 4.14 kN and 2300 mm, respectively. The substantially higher tip deflection of the flax blade is proof of its flexibility. The mean flexural rigidity of the flax and E-glass blades is 24.6 kNm² and 43.4 kNm². While it is demonstrated that the absolute and specific properties of the composites (i.e. flat laminate plaque) are transferred to the blade (i.e. component/structure), it is argued that there is a critical trade-off between component weight savings and component stiffness; for similar stiffness performance of a flax blade to an E-glass blade, weight savings cannot be achieved. Furthermore, while increasing the flax fibre content to enhance the stiffness of the flax blade stiffness may be an attractive option, this would have a substantial detrimental impact on the economic cost and eco-impact of the flax blade.

In conclusion, it is proposed that flax is a suitable structural replacement to E-glass for similar composite small wind turbine blade applications. In view of the findings of this research, it is suggested that i) the development of low-cost sustainable aligned plant fibre semi-products is a limiting factor to the industrial uptake of PFRPs in structural applications, ii) more ambitious studies are required to of **PFRPs** understand the behaviour when employed in specific applications/structures, rather than limiting materials analysis to data extracted from coupon testing, and iii) the development of bio-based high-performance matrix materials and core materials is a critical step in the wide acceptance of PFRPs as sustainable materials.

7.5 REFERENCES

- 1. Reux F. Worldwide composites market: Main trends of the composites industry, in *5th Innovative Composites Summit JEC ASIA 2012*. 26-28 June 2012. Singapore.
- 2. Pickering K, ed. *Properties and performance of natural-fibre composites.* 2008. CRC Press LLC: Boca Raton.
- 3. Carus M. Bio-composites: Technologies, applications and markets, in 4th International Conference on Sustainable Materials, Polymers and Composites. 6-7 July 2011. Birmingham, UK.
- 4. Carus M, Gahle C. Natural fibre reinforced plastics material with future, 2008. nova-Institut GmbH: Huerth.
- 5. Staiger M, Tucker N. *Natural-fibre composites in structural applications*, in *Properties and performance of natural-fibre composites*, Pickering K, 2008. CRC Press LLC: Boca Raton.
- 6. Auto body made of plastics resists denting under hard blows, in Popular Mechanics Magazine, Dec 1941, Vol 76 No. 6. p. 12.
- 7. A Fighter Fuselage in Synthetic Material, Vol. 34, October 1945. Aero Research Limited: Duxford, Cambridge.
- 8. BS EN 61400-2:2006, Wind turbines Part 2: Design requirements for small wind turbines, 2006. British Standards Institution: London.
- 9. Goutianos S, Peijs T, Nystrom B, Skrifvars M. Development of flax fibre based textile reinforcements for composite applications. *Applied Composite Materials*, 2006, 13(4): p. 199-215.
- 10. Baets J, Plastria D, Ivens J, Verpoest I. Determination of the optimal flax fibre preparation for use in UD-epoxy composites, in *4th International Conference on Sustainable Materials, Polymers and Composites*. 6-7 July 2011. Birmingham, UK.
- 11. Miao M, Finn N. Conversion of natural fibres into structural composites. *Journal of Textile Engineering*, 2008, 54(6): p. 165-177.
- 12. Jensen F. *Ultimate strength of a large wind turbine blade*. PhD, 2008. Technical University of Denmark: Lyngby, Denmark.
- 13. Brøndsted P, Lilholt H, Lystrup A. Composite materials for wind power turbine blades. *Annual Review of Materials Research*, 2005, 35: p. 505-538.
- 14. Brøndsted P, Holmes JW, Sørensen BF, Jiang Z, Sun Z, Chen X. Evaluation of a bamboo/epoxy composite as a potential material for hybrid wind turbine blades, 2008. Chinese Wind Energy Association.
- 15. Qin Y, Xu J, Zhang Y. Bamboo as a potential material used for windmill turbine blades A life cycle analysis with sustainable perspective, 2009. Roskilde University Center: Denmark.
- 16. Frohnapfel P, Muggenhamer M, Schlögl C, Drechsler K. Natural fibre composites for innovative small scale wind turbine blades, in *International Workshop on Small Scale Wind Energy for Developing Countries*. 15-17 November 2010. Pokhara, Nepal.
- 17. Mikkelsen L, Bottoli F, Pignatti L, Andersen TL, Madsen B. Material selection and design aspects of small wind turbine blades, in *Indo-Danish Workshop on Future Composites Technologies for Wind Turbine Blades*. 2012. Delhi, India.
- 18. Bottoli F, Pignatti L. Design and processing of structural components in biocomposite materials Rotor blade for wind turbine cars, ed. Madsen B, Mikkelsen LP, Brondsted P, Andersen TL, 2011. Technical University of Denmark: Roskilde, Denmark.
- 19. , Small Wind Systems UK Market Report, 2011. RenewableUK (BWEA): London.

- 20. Hogg P. Wind Turbine Blade Materials, 2010. SUPERGEN WindWind Energy Technology.
- 21. BS-EN 61400-23:2002, Wind turbine generator systems Part 23: Full-scale structural testing of rotor blades, 2002. British Standards Institution: London.
- 22. Shah D, Schubel PJ, Clifford MJ, Licence P. Fatigue characterisation of plant fibre composites for small-scale wind turbine blade applications, in *5th Innovative Composites Summit JEC Asia 2012*. 26-28 June 2012. Singapore.
- 23. Shah D, Schubel PJ, Clifford MJ, Licence P. Fatigue characterisation of plant fibre composites for rotor blade applications, in JEC Composites Magazine, No. 73: Special JEC Asia, June 2012. JEC Composites: Paris. p. 51-54.
- 24. Aziz S, Gale J, Ebrahimpour A, Schoen MP. Passive control of a wind turbine blade using composite material, in *ASME 2011 International Mechanical Engineering Congress & Exposition (IMECE2011)*. November 11-17, 2011. Denver, Colorado, USA.
- 25. Harris B. *Engineering composite materials*, 1999. London: The Institute of Materials.
- 26. Bos H, van den Oever MJA, Peters OCJJ. Tensile and compressive properties of flax fibres for natural fibre reinforced composites. *Journal of Materials Science*, 2002, 37: p. 1683-1692.
- 27. Lewin M. *Handbook of fiber chemistry*. Third ed, 2007. Boca Raton: CRC Press LLC.
- 28. Dittenber D, Gangarao HVS. Critical review of recent publications on use of natural composites in infrastructure. *Composites Part A: Applied Science and Manufacturing*, 2012, 43: p. 1419-1429.
- 29. Madsen B. *Properties of plant fibre yarn polymer composites An experimental study*. PhD, 2004. Technical University of Denmark: Lyngby, Denmark.
- 30. Andserson J, Jansz A, Steele K, Thistlethwaite P, Bishop G, Black A. Green guide to composites an environmental profiling system for composite materials and products, 2004. Building Research Establishment (BRE) and NetComposites: Watford, UK.
- 31. Joshi S, Drzal LT, Mohanty AK, Arora S. Are natural fiber composites environmentally superior to glass fiber reinforced composites? *Composites Part A: Applied Science and Manufacturing*, 2004, 35: p. 371-376.
- 32. Dissanayake N, Summerscales J, Grove SM, Singh MM. Life cycle impact assessment of flax fibre for the reinforcement of composites. *Journal of Biobased Materials and Bioenergy*, 2009, 3(3): p. 1-4.
- 33. Dissanayake N, Summerscales J, Grove SM, Singh MM. Energy use in the production of flax fiber for the reinforcement of composites. *Journal of Natural Fibers*, 2009, 6(4): p. 331-346.
- 34. Summerscales J, Dissanayake N, Virk AS, Hall W. A review of bast fibres and their composites. Part 2 Composites. *Composites Part A: Applied Science and Manufacturing*, 2010, 41(10): p. 1336-1344.
- 35. Steger J. Light weight! No matter what the costs? Plant fibres for light weight automotive applications. *Journal of Biobased Materials and Bioenergy*, 2010, 4(2): p. 181-184.
- 36. Le Duigou A, Davies, P, Baley, C. Environmental impact analysis of the production of flax fibres to be used as composite material reinforcement. *Journal of Biobased Materials and Bioenergy*, 2011, 5(1): p. 153-165.
- 37. Duflou J, Deng Y, Acker KV, Dewulf W. Do fiber-reinforced polymer composites provide environmentally benign alternatives? A life-cycle-assessment-based study. *MRS Bulletin*, 2012, 37: p. 374-382.

- 38. Shah D, Schubel PJ. *Full-scale structural testing of a rotor blade*, 2012. The University of Nottingham: Nottingham.
- 39. Wacker G. Requirements for the certification of rotor blades, in SAMPE 2003 Advancing materials in the global economy Applications, emerging markets and evolving technologies. May 11-15, 2003. Long Beach, California.
- 40. Kalia S, Kaith BS, Kaur I. Pretreatments of natural fibers and their application as reinforcing material in polymer composites a review. *Polymer Engineering and Science*, 2009, 49(7): p. 1253-1272.
- 41. Wambua P, Ivens J, Verpoest I. Natural fibres: can they replace glass in fibre reinforced plastics? *Composites Science and Technology*, 2003, 63: p. 1259-1264.
- 42. Hughes M, Carpenter J, Hill C. Deformation and fracture behaviour of flax fibre reinforced thermosetting polymer matrix composites. *Journal of Materials Science*, 2007, 42: p. 2499-2511.
- 43. Baley C. Analysis of the flax fibres tensile behaviour and analysis of the tensile stiffness increase. *Composites Part A: Applied Science and Manufacturing*, 2002, 33: p. 939-948.
- 44. McKittrick L, Cairns DS, Mandell J, Combs DC, Rabern DA, van Luchene RD. *SAND2001-1441*, Analysis of a composite blade design for the AOC 15/50 wind turbine using a finite element model, 2001. Sandia National Laboratories: Livermore, California.
- Bos H, Molenveld K, Teunissen W, van Wingerde AM, van Delft DRV. Compressive behaviour of unidirectional flax fibre reinforced composites. *Journal of Materials Science*, 2004, 39: p. 2159-2168.